INSTITUTE FOR DEFENSE ANALYSES

Change Detection Using Down-Looking Ground-Penetrating Radar

Elizabeth L. Ayers
Eric Bressler
Marie E. Fishel
Erik M. Rosen

April 2014

IDA Document NS D-5154
Log: H 14-000295

INSTITUTE FOR DEFENSE ANALYSES
4850 Mark Center Drive
Alexandria, Virginia 22311-1882

The Institute for Defense Analyses is a non-profit corporation that operates three federally funded research and development centers to provide objective analyses of national security issues, particularly those requiring scientific and technical expertise, and conduct related research on other national challenges.

About This Publication
This work was conducted by the Institute for Defense Analyses (IDA) under contract HQ0034-14-D-0001 Project AK-2-1997, "Test Design and Analysis Support for the Development of Vehicle-Based Mine and IED Detection Systems," for the Office of the Assistant Secretary of Defense, Research and Engineering/Research Directorate (ASD(R&E)), and the U.S. Army Communication Electronics Command (CECOM), Night Vision Electronic Sensors Directorate (NVESD), Countermine Division, Ground Vehicles Application Branch. The views, opinions, and findings should not be construed as representing the official position of either the Department of Defense or the sponsoring organization.

Change Detection Using Down-Looking Ground-Penetrating Radar

Elizabeth Ayers[a], Eric Bressler[a], Marie Fishel[a], Erik M. Rosen[a]
[a]Institute for Defense Analyses, 4850 Mark Center Drive, Alexandria, VA 22311

ABSTRACT

Down-looking ground-penetrating radar (DLGPR) has been used extensively for buried target detection. For operational implementations, the sensor is used in direct-detection mode, where algorithms process data while the system moves down roadways. Decisions are made before a system passes over the target. Change detection works by passing over an area before and after targets are buried. By comparing before-and-after data, change detection can improve DLGPR performance, but it also has inherent operational limitations. Performance enhancements include mitigating the effects of anomalies not associated with targets and increasing the detection probabilities of deeper targets through indirect means. In the latter case, deeply buried targets that do not appear in the GPR data can be indirectly detected using change-detection methods if the patch of ground where the target is buried has been significantly modified from its original undisturbed state. In this paper, we explore decision-based change-detection approaches for enhancing the performance of a DLGPR system and enumerate the limitations of the approach.

Keywords: change detection, down-looking ground-penetrating radar, DLGPR, mine detection

1. INTRODUCTION

Most of the down-looking ground penetrating radar (DLGPR) systems employed for buried target detection have concentrated on the problem of directly detecting the anomaly in the GPR data caused by the buried object. Furthermore, most DLGPR algorithms attempt to reduce false-alarm rates through some form of discrimination, in which features are extracted and classifiers are trained on known targets and false alarms[1]. With change detection, feature extraction and classification are de-emphasized, the reductions in false alarms resulting instead from comparisons of the ground before and after targets are buried.

For DLGPR systems, the largest response is typically due to the radar reflecting off the ground. Most DLGPR algorithms remove the ground-bounce response as a first pre-processing step. The remaining subsurface response is then used to detect buried targets. DLGPR systems are not able to detect some targets due to the soil conditions in which they are buried, the depth at which they are buried, or both. Those targets simply do not show up in the subsurface response of the radar. But when the ground is scanned before the targets are buried, change detection can be used to indirectly detect targets that otherwise cannot be detected directly. Despite some operational limitations imposed on the implementation of change detection, the approach can still be assessed for its efficacy. In this paper, we apply various algorithms to data collected in support of a change-detection test. Sample GPR data associated with algorithm outputs sheds light on the process. We provide receiver operator characteristic (ROC) curves that demonstrate enhanced performance using change detection.

2. LIMITATIONS OF CHANGE DETECTION

The change-detection results and conclusions presented in this paper are encouraging but have many limitations that must be overcome before these techniques can be used in the field. Limitations of implementing change detection for DLGPR systems include a reliance on differential Global Positioning System (DGPS) to accurately correlate alarms from one excursion to another, the misidentification of changes in the soil, and logistical implementation hurdles.

The results presented in this paper are derived from data collected using real-time kinematic (RTK) DGPS, which is accurate to a few centimeters. RTK-DGPS requires the use of a base station at known, surveyed locations, with radios transmitting differential corrections from the base station to a receiver on the moving DLGPR system. The resulting accuracy of the alarm positions allows for the correct association of alarms caused by the same subsurface source—from one excursion to another or from one day to another. The required accuracy of the alarm positions is in part determined by the size of the targets that the system is designed to detect. Since the targets are typically less than 1/2 meter in size, linking distances are approximately the same length. If a GPS system without differential corrections was used to

compute alarm locations with an accuracy of a meter or more, it would be difficult to accurately link an alarm due to a subsurface object from one excursion to another. At such accuracy, an alarm from a subsurface object could be reported as far away as several meters from an alarm from the same subsurface object generated from a prior excursion. Although some types of navigation systems can enhance the accuracy of GPS systems that do not benefit from differential corrections, these are not considered here.

Alarms produced by automatic target recognition (ATR) algorithms on board the DLGPR system depend on soil conditions. It is therefore expected that change detection using DLGPR systems will suffer from high false-alarm rates when soil conditions vary from one excursion to another. For example, if the soil is dry one day and moist the next, the alarms generated by the ATR can differ significantly in number and in confidence value. As a result, many alarms will not have a natural match from one excursion to another. Change detection requires at least a match in alarm locations and sometimes requires that alarm confidence values be nearly the same. In conditions in which roadways are traveled by vehicular or foot traffic, it is expected that the impact on the soil conditions of the road surface and shallow subsurface will change from day to day, or from hour to hour. These changes can potentially give rise to alarms even though they have nothing to do with buried targets.

To implement change detection into roadway-monitoring scenarios, the alarms from all excursions must be accurately shared between each of the DLGPR vehicles. This requirement imposes a strict set of protocols to be followed. The effectiveness of change detection relies on the continual monitoring of a given roadway, which places additional logistical burdens on those responsible for monitoring the road.

3. DLGPR DATA FUNDAMENTALS

To evaluate various approaches to direct detection and change detection, we study the sensor data in their fundamental forms, adopting the terminology used in Daniels book on GPR[2]. The fundamental response of any DLGPR system is the A-scan, which is associated with a particular down-track location and a particular across-track channel. When we examine DLGPR data from most systems, we typically differentiate raw A-scans from processed A-scans. Figure 1 shows an A-scan response collected over a buried metallic target. The largest response is from the ground, followed by two distinct high-magnitude reflections from the target itself. Nearly all other parts of the response are zero, including the response before the ground bounce, the response between the ground and the buried target, and the response after (or deeper) than the buried target.

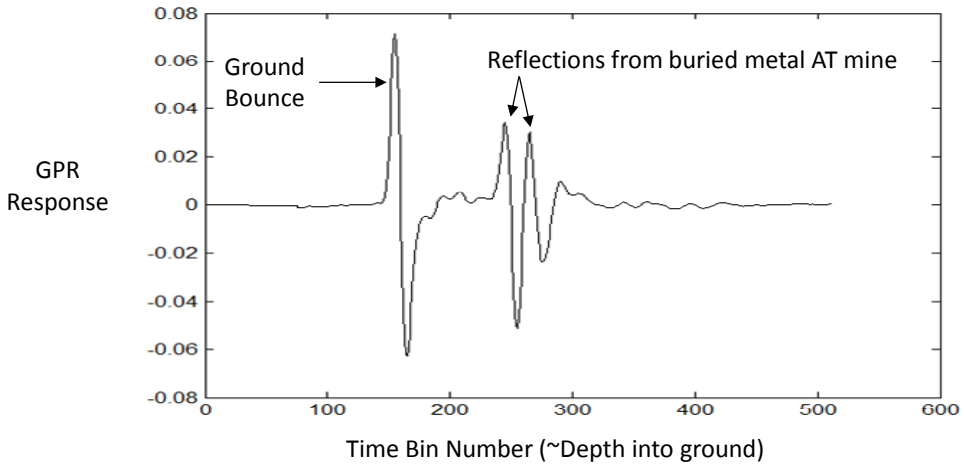

Figure 1. DLGPR A-scan for a buried metallic target.

If we rotate the A-scan of figure 1 90 degrees so that the ground bounce is at the top and then plot neighboring A-scans to the left and right of it, we get the resultant waterfall plot shown in figure 2. There are 51 across-track channels in this particular DLGPR system. All the A-scans of figure 2 come from channel 40, which happens to be the channel in which the target is centered. Thus, the adjacent A-scans are from successive along-track scans, which are spaced approximately

every 0.05 meters. In figure 2, the *x*-axis is the local scan number, and so the 51 A-scans shown were collected over about 2.5 meters of along-track distance. (We use the terms along-track and down-track interchangeably).

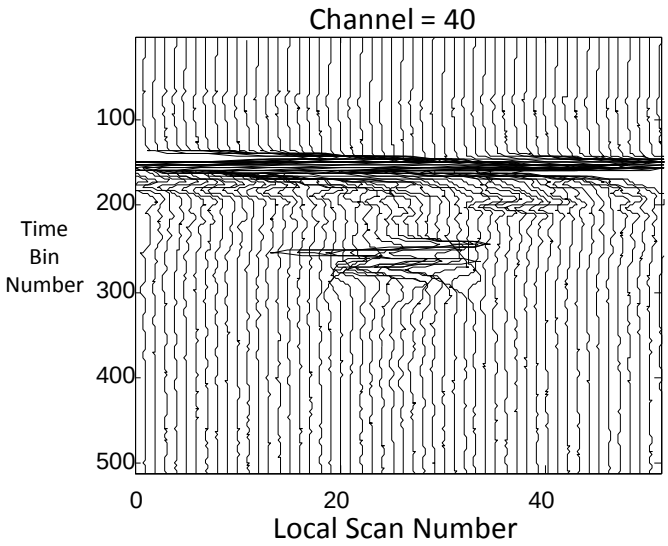

Figure 2. DLGPR waterfall plot of A-scans for a buried metallic target.

If instead of plotting *x*–*y* A-scans, we create a grayscale image of the GPR responses, we get an along-track B-scan, as shown in figure 3. Here, the peaks and valleys of the GPR responses have been mapped to a color on the gray-scale color bar, with white being a high-magnitude peak and black being a high-magnitude valley. We observe that the metallic target manifests itself as a parabola in this B-scan view of the GPR data.

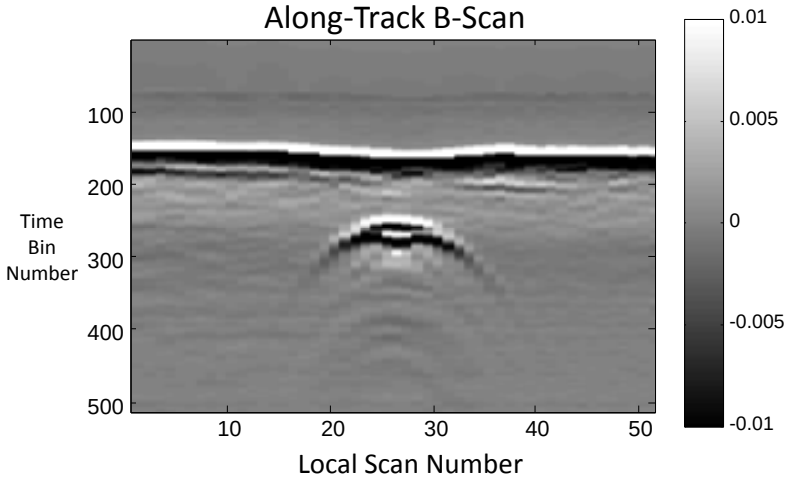

Figure 3. DLGPR along-track B-scan for a buried metallic target.

We now construct a two-dimensional C-scan from the three-dimensional volumetric GPR data. The matrix dimensions of the C-scan are given by the number of down-track scans and by the number of across-track channels. In this way, the C-scan can be thought of as a bird's-eye view of the lane, or roadway, which was scanned by the DLGPR system. The simplest way to generate a C-scan is to take a slice of the three-dimensional GPR data at a fixed depth, or time bin. Alternatively, there are countless ways to transform the three-dimensional GPR data to a two-dimensional C-scan[3]. A common technique is to take the sum of the squares of each A-scan. Other methods include KSum[4], Disturbed Soil Metric[5], and LMS[6]. Figure 4 shows a C-scan corresponding to the same metallic target shown in the B-scan of figure 3,

in this case derived from a variant of the LMS algorithm. Essentially, the volumetric three-dimensional GPR data are processed and collapse to two dimensions. Targets manifest themselves as blobs in the C-scan images, where white pixels are of the highest magnitude and black pixels are of the lowest magnitude.

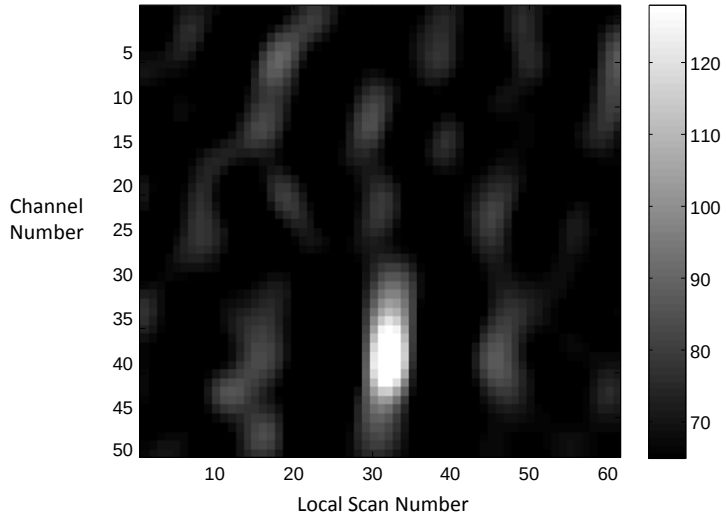

Figure 4. DLGPR C-scan for a buried metallic target.

An illustrative way of presenting the GPR data at a target or alarm location is to show the down-track B-scan, across-track B-scan, and a C-scan projected onto the faces of a cube. Figure 5 shows a DLGPR cube at the location of the buried metallic target. High-intensity blobs in the C-scan are mapped to a color scale where magenta represents the highest magnitude response.

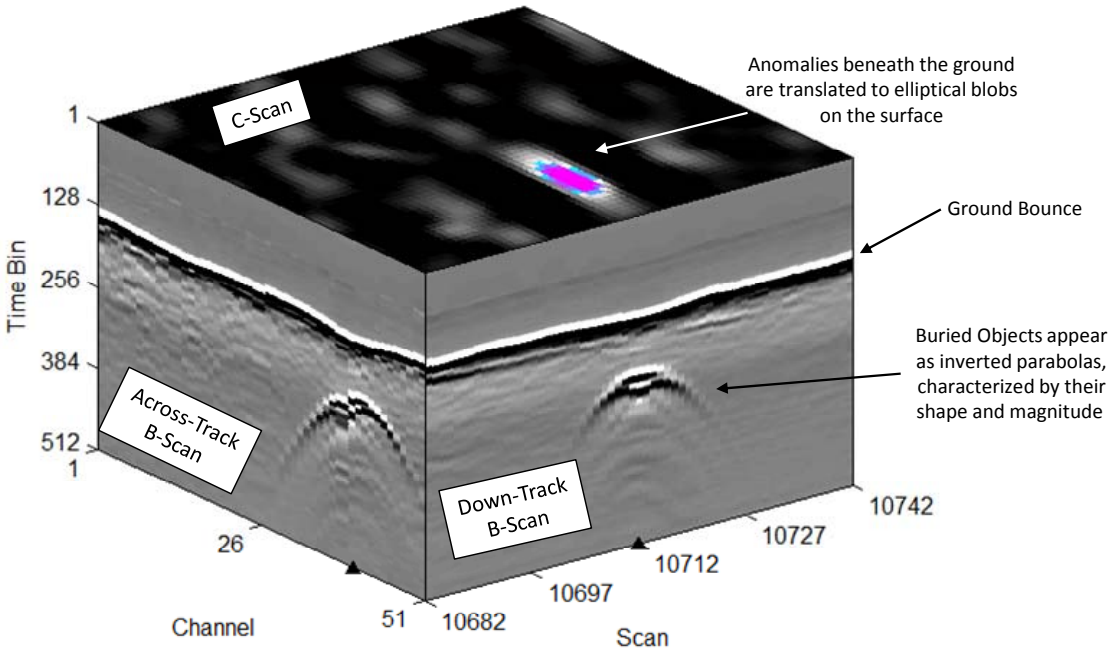

Figure 5. DLGPR cube for a buried metallic target.

4. DECISION-BASED CHANGE DETECTION

4.1 General Approach

In decision-based change detection, alarms are compared from excursions before and after targets are buried. A comparison of their locations is all that is necessary to gain a benefit from this form of change detection. But if we also use the confidence levels of the alarms, we can improve the change-detection result.

Figure 6 depicts the operational and testing scenario that suggests a change-detection approach for detecting buried targets. Each of the sub-figures represents an event in time. In figure 6a, a DLGPR system scans a roadway before any targets are buried. The system generates a list of suspected target locations, or alarms, which are shown as numbers. The essential elements of an alarm are a unique alarm number, a GPS location, and an ATR scalar output—also referred to as a confidence level. The higher the ATR output, the greater the confidence that the alarm is due to a target and not a false alarm. Since no targets were present in the roadway when the system made its first pass, the four alarms in figure 6a are, by default, false alarms. For this analysis, we are not interested in the source of these false alarms. Since no known targets were encountered, the probability of detection (P_D) is not defined.

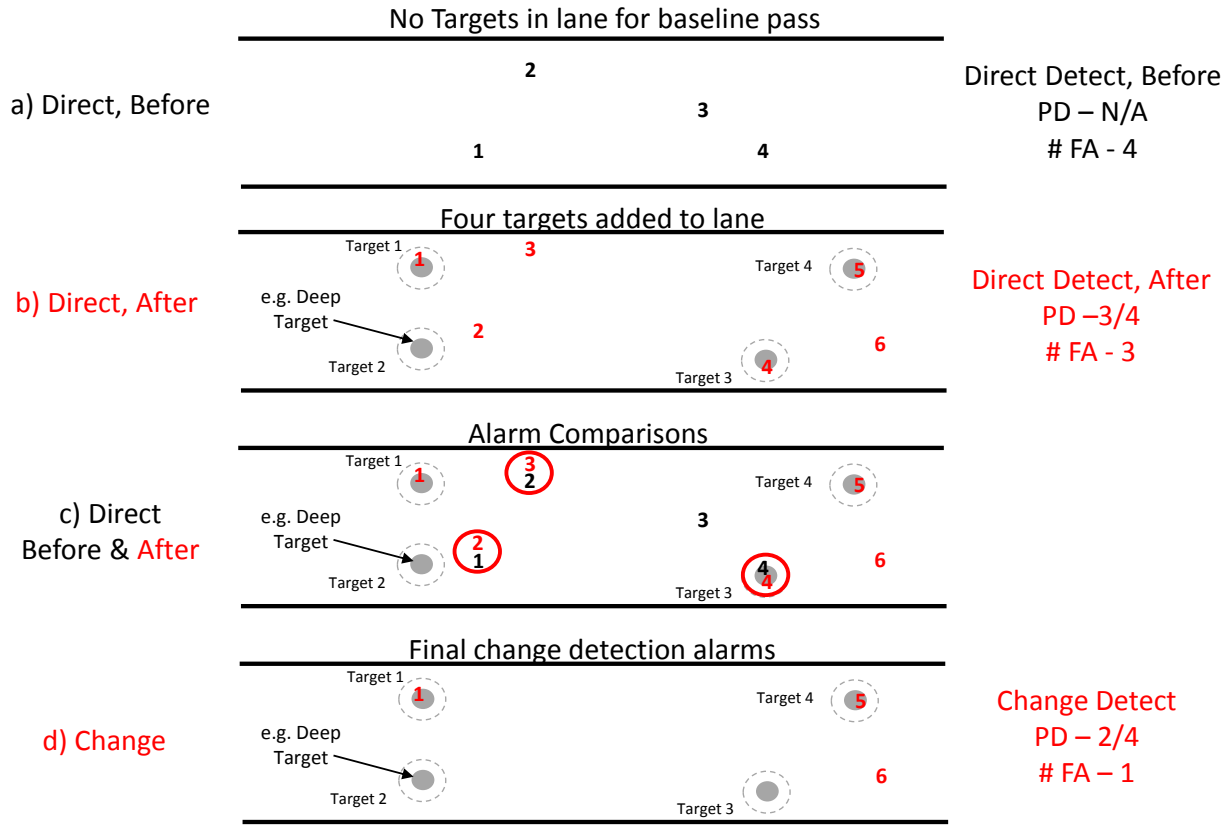

Figure 6. Depiction of change detection approach.

Between the scenarios depicted in figures 6a and 6b, four targets are buried in the roadway. Targets are depicted as gray circles, and the halo radii are depicted as dashed gray circles surrounding the targets. Halo radii are the allowable miss distances between an alarm and a target. Alarms within the halo of a target are deemed detections, and alarms outside the halos are deemed false alarms. In figure 6b, we see the result of a second pass by the DLGPR system. A new set of alarms is generated, this time represented by numbers in red. After targets are buried, a total of six alarms are generated by the direct detection algorithm of the DLGPR system. We see in figure 6b that alarms 1, 4, and 5 fall within the halo of three of the four targets, but alarms 2, 3, and 6 fall outside the halos of the targets. Target 2 is not detected (it could be a deeply buried target that the system was not designed to detect). The direct-detection result is three out of four targets detected, with three false alarms.

4.2 Change Detection Using Only Locations of Alarms

We now apply change detection by overlaying the alarms from the excursion before targets were buried (black numbers) with the alarms from the excursion after targets were buried (red numbers). The result is shown in figure 6c. For our first attempt at change detection, we compare alarm locations from the second excursion with alarm locations from the first excursion and remove alarms that are spatially correlated. For our analysis, we used a linking distance of 0.5 m. In figure 6c, red circles are placed around alarm pairs that meet the linking-distance criterion. After eliminating spatially correlated alarms, we are left with fewer alarms for the second excursion, as shown by the red numbers in figure 6d. For our initial approach, we do not retain any of the alarms from the first excursion (black numbers). With reference to figure 6d, we see that there are only three remaining alarms. The change-detection result is two out of four targets detected, with one false alarm. For this case, we eliminated two of the three false alarms, but also removed one of the three detections of targets. It is the goal of change detection to reduce the false-alarm rate significantly, with only modest reductions in the probability of detection. Optimally, we would like to eliminate all the false alarms without sacrificing any detections.

4.3 Enhancing Change Detection Performance by Using Alarm Confidence Values

We reexamine what happened with target 3. We see that it was detected in figure 6b, but the alarm from the second excursion (red alarm number 4) was then eliminated by virtue of being near an alarm from the first excursion (black alarm number 4). We might say that alarm number 4 from the first excursion (black number) was *in the wrong place at the wrong time*. How might we modify our change-detection algorithm so that red alarm number 4 is not eliminated? What additional information is at our disposal, other than the location of the alarms? The answer is that we can compare not only the location of first and second excursion alarms, but also their direct-detection algorithm confidence values. If the confidence values of spatially correlated alarms are similar, we proceed to eliminate the second excursion alarms. By doing this, we are essentially saying that the ground has not changed from the first excursion to the second excursion. Whatever subsurface anomaly gave rise to a direct-detection alarm, it appears essentially the same from the first pass to the second pass. That is, these alarms are deemed as arising from the same source, which means that no change occurred in the roadway at these locations. In the case that the confidence value of the second excursion alarm is greater than the confidence value of the first excursion by a certain percentage, we do not remove the second-pass alarm. Here, the assumption is that something changed in the ground to give rise to an alarm with a significantly greater confidence value. For our problem it was the introduction, or burial, of a target. This case is depicted in figure 7, in which the second excursion alarm (red alarm 4) has a confidence value of 9.2, which is deemed significantly greater than the first excursion alarm (black alarm 4), which has a confidence value of 2.1. Figure 8 shows the results of using this enhanced decision-based change-detection algorithm. Now the number of false alarms has been reduced to one, as before, and the number of detections is *restored* to 3.

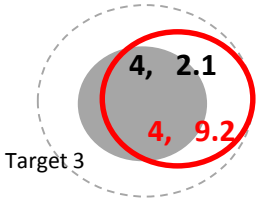

Figure 7. Alarm numbers and confidences associated with target 4.

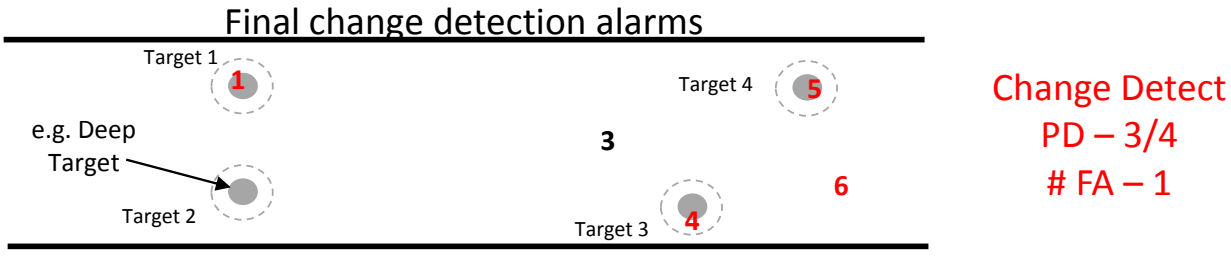

Figure 8. Depiction of change detection result when alarm confidence is used, in addition to alarm location.

We now turn to the case of target 2, which we suppose is a deeply buried target that the DLGPR cannot detect directly. Using change detection, are there means by which deeply buried targets can be detected indirectly by virtue of comparisons of the same patch of ground before and after the target is buried? Does the GPR data hold more clues or evidence of a deeply buried target, other than the typical direct-detection approach of detecting and discriminating hyperbolic anomalies? In the next section, we examine one such method.

5. CHANGE DETECTION USING GROUND-BOUNCE METRIC

A metric was developed to identify a specific phenomenon that sometimes occurs when targets are buried. The phenomenon can be particularly pronounced for deeply buried targets since they tend to require a larger hole to be dug than smaller targets. The metric allows the system to indirectly detect deeply buried targets, which likely cannot be directly detected by the GPR. The metric can be implemented as a change-detection method, where the current view of the ground is examined and compared to the ground at the same location at a previous time, or as a direct-detection method, where only the current view of the ground is analyzed.

Figure 9 depicts the phenomenon that the metric was created to detect. The set of B-scans on the left correspond to a location traversed by a DLGPR without a target present. The B-scans on the right correspond to the same location after a target was buried at a deep depth. Physics limitations prevent the DLGPR from receiving a response from a target this deep, and thus the target cannot be seen in the B-scan images. But there is evidence of the target burial when the ground-bounce location is examined. On the left, the ground is relatively flat in the down-track B-scan and almost completely flat in the across-track B-scan. After the target is buried, a depression is centered at the target location, as shown in the B-scans on the right.

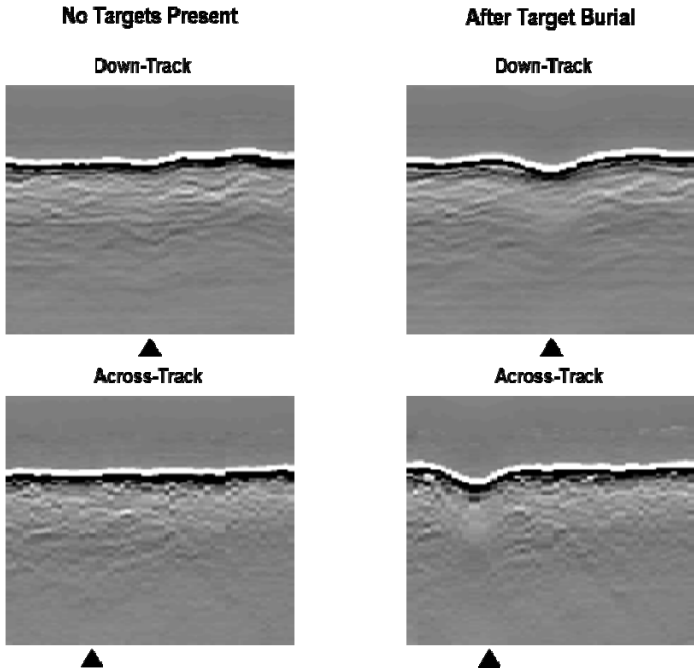

Figure 9. Across-track and down-track B-scans of a location before and after target burial.

The aptly named *ground-bounce metric* utilizes ground-bounce location information to attempt to identify the scenario where there is a depression at the location of a deeply buried target. Unlike the previous decision-based change-detection methods, this metric is a stand-alone routine applied to three-dimensional GPR data to create alarm files that can be fused with other pre-screener alarm files in hopes of attaining a better overall ROC curve due to the additional detections of deeply buried targets.

The algorithm begins by calculating the ground-bounce location for every channel at each down-track scan, creating a two-dimensional C-scan map of these values. Here, the ground-bounce location is defined as the time bin number corresponding to the maximum radar amplitude response due to the ground bounce. If the algorithm is being utilized as a change-detection method, then C-scan maps of ground-bounce locations are created for the GPR data *before* and *after* targets are buried. To account for differing antenna heights at the same down-track location *before* and *after* targets are buried, the algorithm calculates the mean ground-bounce value for all channels in each down-track scan. The algorithm then subtracts each ground-bounce location in the C-scan map from the mean ground-bounce location corresponding to that particular down-track scan. If the algorithm is being applied as a change-detection method, the C-scan map from *before* the target is buried is used to calculate the mean ground-bounce location, and the C-scan map corresponding to *after* the target is buried is subtracted from the mean. This method could also be utilized as direct detection of disturbed earth by only examining the C-scan corresponding to after the target is buried. In this case, the algorithm calculates the mean ground-bounce location of all channels in a down-track scan and then subtracts the ground-bounce values at every channel in the same scan from this location.

A Prewitt filter is applied to the resultant C-scan to eliminate striping and utilize edge-detection features to enhance responses due to depressions. Figure 10 shows C-scans for the same location pictured in Figure 9 where a target was buried at a deep depth. The C-scan map on the left was created by subtracting the ground-bounce location at each channel and down-track scan from the mean ground-bounce location at that down-track scan. The resulting C-scan contains vertical striping, which is removed by applying a Prewitt filter. The effects of applying the Prewitt filter can be seen in the C-scan map on the right; the striping is gone and the location of the recently buried target stands out as a bright spot compared against the background.

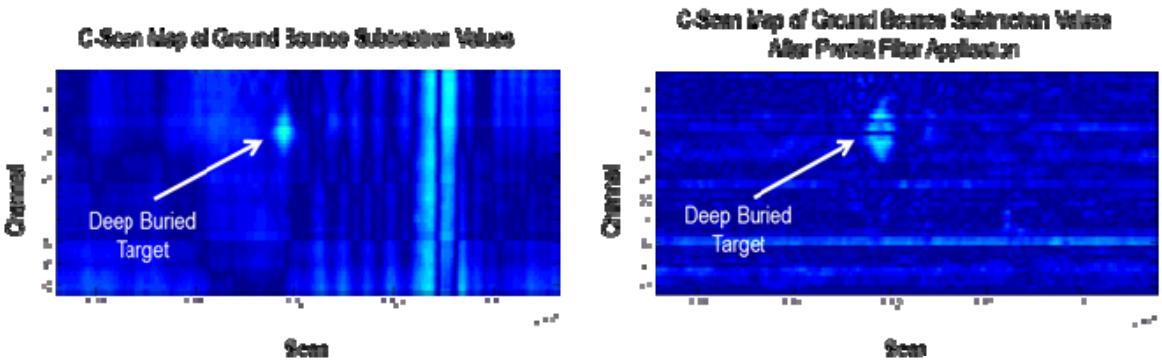

Figure 10. C-scan maps.

Alarm files are created from the filtered C-scan map by applying a threshold to the image and looking for areas where five or more adjacent pixels have values above threshold. Figure 11 is a flowchart that outlines the entire procedure by which the ground-bounce metric is applied to the GPR data to create alarm files.

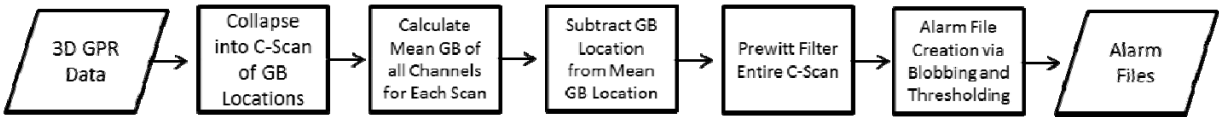

Figure 11. Flowchart depicting how alarm files are created using the disturbed soil metric.

6. RESULTS

Figure 12 gives ROC curves for the change-detection approaches and algorithms portrayed in figures 6 through 8. The part of the ROC curve shown in figure 12 is deemed to be of operational interest. If the false-alarm rate (FAR) is any higher, it is expected that the system would not be embraced as a tool for target detection because the system would need to stop too frequently at locations where no targets were buried. Error bars on P_D are represented by fainter colored lines. We see that when using only the location of the alarms, the change-detection approach enhances detection performance at low false-alarm rates. For a FAR of 0.001 m^{-2}, the P_D for direct detection is about 0.55 (black curve), while for change

detection it is about 0.65 (blue curve). But at a higher FAR of 0.006 m^{-2}, the P_D for change detection (using only location of alarms) is lower than the P_D for direct detection. The benefit of eliminating false alarms with change detection is offset by a reduction in P_D at a FAR of 0.006 m^{-2}. But when we also utilize the confidence values of the alarms we improve the change-detection result. By accounting for some cases in which an alarm was *in the wrong place at the wrong time* (see alarm number 4 in figure 6a), the P_D at 0.001 m^{-2} increases from 0.65 to about 0.70, and at the higher FAR of 0.006 m^{-2}, no degradation in P_D is seen. The value of change detection is evident when we compare the FARs at a fixed P_D. Using only direct detection, we see that the ROC curve reaches its final plateau (for the false-alarm regime shown in figure 12), or its maximum P_D of about 0.70, at a false-alarm rate of 0.004 m^{-2}. But by using change detection (using location and confidence values), a P_D of 0.70 is realized at a false-alarm rate of only 0.001 m^{-2}. The number of false alarms is reduced by a factor of 4. This has implications for fielded DLGPR systems. If the limitations of using change detection in a fielded system can be overcome, there is a potential for delivering detection performance as much lower false-alarm rates, such that system thresholds can be changed accordingly, and operational tempos can be dramatically increased.

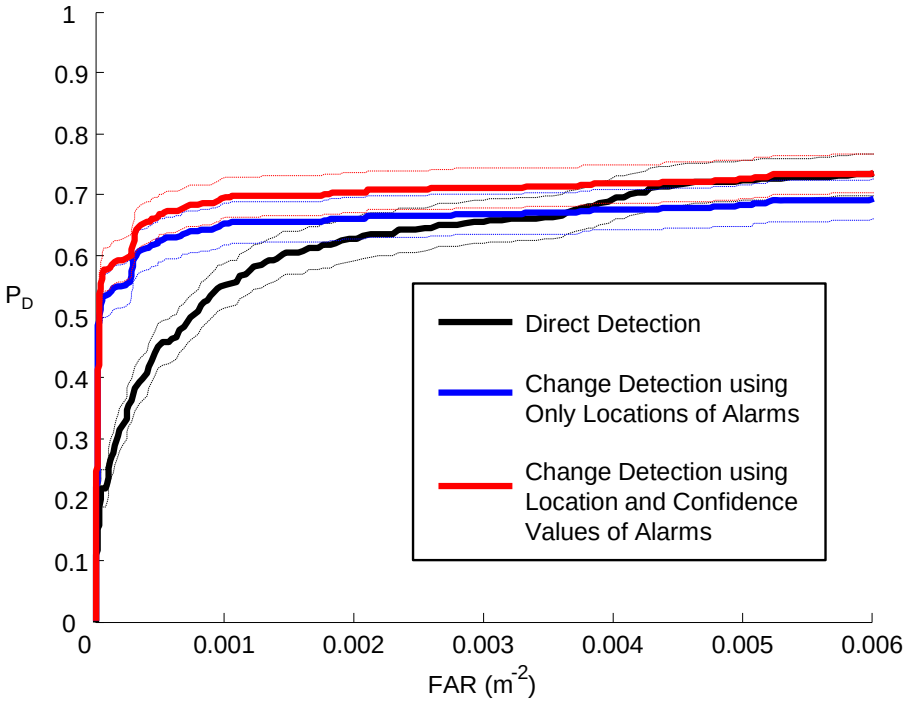

Figure 12. Direct-detection results (black curve), change-detection results using location-only (blue curve), and change-detection results using location and confidence values of alarms (red curve), for all test lanes.

We are still left with a ROC curve that plateaus at a P_D of 0.70. This performance is primarily due to the limitations of the GPR sensor, which in this case was not designed to detect deeply buried targets. By employing the ground-bounce metric described in section 5, we see potential for the indirect detection of deeply buried targets. Figure 13 shows ROC curves for deep targets, limited to one test lane. Here, the ground-bounce metric applied in a change-detection sense greatly enhances detection of deeply buried targets. Direct detection results in a P_D of zero (black curve is aligned with the *x*-axis), and application of the ground-bounce metric results in the detection of half the deeply buried targets. It remains to be seen if the technique is robust when applied to the larger data set. The data used for the ROC curve in figure 13 did not include some of the rougher lanes, which could induce false alarms due to greater variance in the ground-bounce locations from run to run.

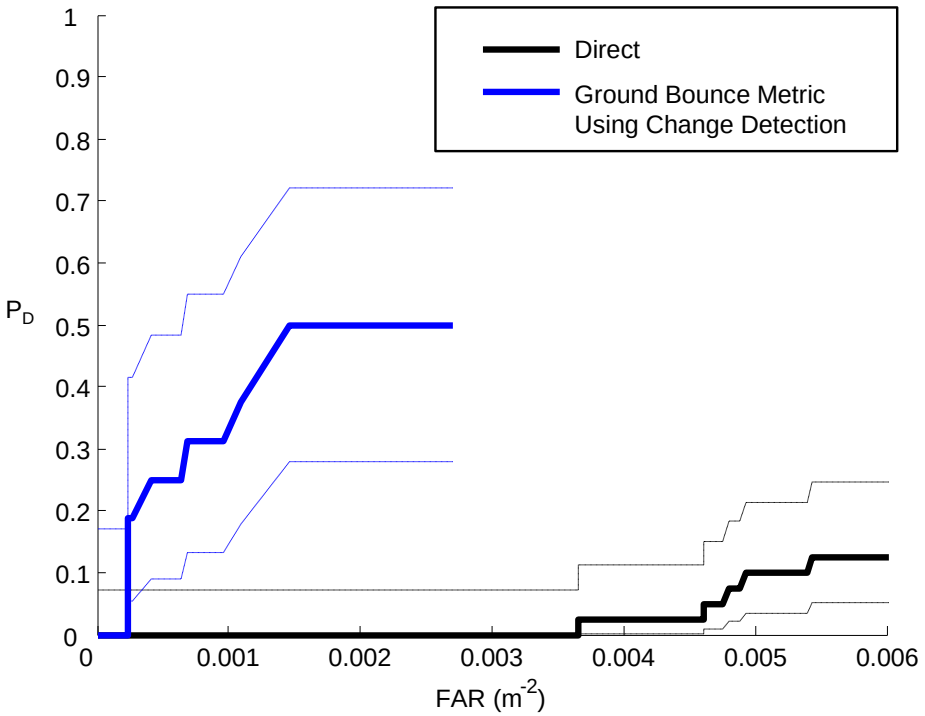

Figure 13. ROC curves for deep targets, limited to one test lane.

7. CONCLUSIONS

Although employing change detection in locations where high-accuracy GPS is denied is fraught with technical challenges, the results in this paper indicate that applying change detection to DLGPR systems has the potential to enhance detection performance. By utilizing techniques that indirectly detect deeply buried targets, detection performance can potentially be enhanced against the entire target set.

8. FUTURE WORK

The next step is to fuse the ground-bounce metric alarms with other pre-screener alarms to enhance overall detection performance. The goal is to increase the P_D plateau of figure 12 without incurring a false-alarm penalty that ultimately degrades detection performance. One idea is to leverage a phenomenon in which deeply buried targets give rise to a sort of blurred effect in the three-dimensional GPR data. In these cases, subsurface clutter is destroyed when the target is buried deeply, and thus the amount of subsurface energy actually decreases when the target is buried. This would lead to local anomaly nulls, rather than peaks.

REFERENCES

[1] Wilson, J. N., Gader, P., Lee, W., Frigui, H. and Ho, K. C. “A large-scale systematic evaluation of algorithms using ground-penetrating radar for landmine detection and discrimination,” IEEE Transactions on Geoscience and Remote Sensing 45(8), 2560-2572 (2007).

[2] Daniels, D. J. [Ground Penetrating Radar, 2nd Edition], The Institution of Engineering and Technology (2004).

[3] van Kempen, L. and Sahli, H., “Ground penetrating radar data processing: A selective survey of the state of the art literature,” Technical Report, IRIS-TR-0060, Department of Electronics and Information Processing, Vrije Universiteit Brussel (1999).

[4] Rosen, E. M., “Assessment of down-looking GPR sensors for landmine detection,” Proc. SPIE 5794, 423, (2005).

[5] Rosen, E. M., “Fusion of disturbed soil feature for down-looking ground penetrating radar mine detection,” Proc. SPIE 6553, 1-10 (2007).
[6] Torrione, P., Collins, L. Clodfelter, F., Frasier, S. and Starnes, I. “Application of the LMS algorithm detection using the Wichmann/Niitek ground penetrating radar,” Proc. SPIE 5089, 1127-1136, (2003).

REPORT DOCUMENTATION PAGE

Form Approved
OMB No. 0704-0188

PLEASE DO NOT RETURN YOUR FORM TO THE ABOVE ADDRESS.

1. REPORT DATE	2. REPORT TYPE	3. DATES COVERED *(From–To)*
April 2014	Final	September 2013 – March 2014

4. TITLE AND SUBTITLE

Change Detection Using Down-Looking Ground-Penetrating Radar

5a. CONTRACT NUMBER
HQ0034-14-D-0001

5b. GRANT NUMBER

5c. PROGRAM ELEMENT NUMBER

6. AUTHOR(S)

Ayers, Elizabeth L.
Bressler, Eric
Fishel, Marie E.
Rosen, Erik M.

5d. PROJECT NUMBER

5e. TASK NUMBER
AK-2-1997

5f. WORK UNIT NUMBER

7. PERFORMING ORGANIZATION NAME(S) AND ADDRESS(ES)

Institute for Defense Analyses
4850 Mark Center Drive
Alexandria, VA 22311-1882

8. PERFORMING ORGANIZATION REPORT NUMBER

IDA Document NS D-5154
Log: H 14-000295

9. SPONSORING / MONITORING AGENCY NAME(S) AND ADDRESS(ES)

U.S. Army Communication Electronics Command (CECOM)
Night Vision Electronic Sensors Directorate (NVESD)
Countermine Division
Ground Vehicles Application Branch
10221 Burbeck Road
Ft. Belvoir, VA 22060-5806

10. SPONSOR/MONITOR'S ACRONYM(S)

CECOM/NVESD

11. SPONSOR/MONITOR'S REPORT NUMBER(S)

12. DISTRIBUTION/AVAILABILITY STATEMENT

Approved for public release; distribution is unlimited (1 April 2014).

13. SUPPLEMENTARY NOTES

14. ABSTRACT

Down-looking ground-penetrating radar (DLGPR) has been used extensively for buried target detection. For operational implementations, the sensor is used in direct-detection mode, where algorithms process data while the system moves down roadways. Decisions are made before a system passes over the target. Change detection works by passing over an area before and after targets are buried. By comparing before-and-after data, change detection can improve DLGPR performance, but it also has inherent operational limitations. Performance enhancements include mitigating the effects of anomalies not associated with targets and increasing the detection probabilities of deeper targets through indirect means. In the latter case, deeply buried targets that do not appear in the GPR data can be indirectly detected using change-detection methods if the patch of ground where the target is buried has been significantly modified from its original undisturbed state. In this paper, we explore decision-based change-detection approaches for enhancing the performance of a DLGPR system and enumerate the limitations of the approach.

15. SUBJECT TERMS

change detection, down-looking ground-penetrating radar, DLGPR, mine detection

16. SECURITY CLASSIFICATION OF:			17. LIMITATION OF ABSTRACT	18. NUMBER OF PAGES	19a. NAME OF RESPONSIBLE PERSON
					Barlow, Brian
a. REPORT	b. ABSTRACT	c. THIS PAGE			19b. TELEPHONE NUMBER *(include area code)*
Uncl.	Uncl.	Uncl.	SAR	15	(703) 704-2664

Standard Form 298 (Rev. 8-98)
Prescribed by ANSI Std. Z39.18